Journal of Solid State Chemistry 184 (2011) 2738–2743

Contents lists available at SciVerse ScienceDirect

Journal of Solid State Chemistry

journal homepage: www.elsevier.com/locate/jssc

Preparation of nickel oxide and carbon nanosheet array and its application in glucose sensing

Xin Li [a,b], Anzheng Hu [a], Jian Jiang [a], Ruimin Ding [a], Jinping Liu [a], Xintang Huang [a,*]

[a] Center for Nanoscience and Nanotechnology, Central China Normal University, Wuhan 430079, China
[b] Department of Applied Physics, Wuhan University of Science and Technology, Wuhan 430081, China

ARTICLE INFO

Article history:
Received 9 March 2011
Received in revised form
25 July 2011
Accepted 10 August 2011
Available online 22 August 2011

Keywords:
Nickel oxide
Nanosheet array
Carbon
Hydrothermal method
Glucose sensing

ABSTRACT

Nickel oxide and carbon (NiO/C) nanosheet array was fabricated on Ti foil for the first time by calcining the precursor, which was synthesized through the hydrothermal reaction of nickel acetate, urea and glucose. The slow release of OH^- by the hydrolysis of urea aided in the direct nucleation and adhesion of precursor seeds on Ti substrate. The presence of carbon ensured a large specific surface area and good conductivity of the final NiO/C composite. The prepared NiO/C nanosheet array exhibited higher catalytic oxidation activity of glucose compared with the pure NiO nanosheet at a detection limit of 2 μM, linear range up to 2.6 mM (R^2=0.99961), and sensitivity of 582.6 μA M^{-1} cm^{-2}. With good analytical performance, simple preparation and low cost, this composite is promising for nonenzymatic glucose sensing.

1. Introduction

Glucose determination has attracted considerable interest in biotechnology, clinical diagnostics and the food industry [1]. A number of studies have focused on developing electrochemical glucose sensors over the past few decades [2] and enzymatic glucose biosensors with good selectivity and sensitivity have been successfully developed [3,4]. However, these biosensors lack long-term stability [5]. Thus, different nonenzymatic glucose sensors should be explored [6–10].

Nonenzymatic electro-oxidation of glucose using Ni-based material has been extensively studied, since Fleishman and his co-workers [11] demonstrated that organic compounds could be partially oxidized at a nickel anode in alkaline solution. Glucose sensors based on Ni metallic nanomaterials exhibited high catalytic oxidation activity over glucose [12–14]. However, Ni metallic nanomaterials are unstable and easily oxidized in air and solution. Therefore, considerable efforts have been focused on the use of nickel oxide to modify the electrodes. Cheng et al. [15] devised NiO nanoparticles modified carbon paste electrode. Liu et al. [16] prepared Ni/NiO nanoparticle-loaded carbon nanofiber paste electrode. These proposed electrodes exhibited long-term stability towards the glucose determination. However, a common problem that occurred when using NiO to modify electrodes is the poor charge transport.

Carbon materials have received considerable attention because of their unique properties, such as excellent conductivity, high surface area-to-volume ratio, and good physicochemical stability [17]. Carbon nanotubes, diamond like carbon and graphene have been used to improve the conductivity of composite in the glucose determination [18–20]. However, the preparation of these carbon materials is not simple and economy. Considering this point, partially graphitized carbon would be a good substitute. An important example was demonstrated by Huang et al. [21]. The electronic conductivity of NiO/C composite was improved after the incorporation of partially graphitized carbon. The prepared composite exhibited much better performance as lithium-ion battery electrode material than pure NiO. However, to our knowledge, using NiO and partially graphitized carbon composite for nonenzymatic glucose sensing has never been discussed before. Stimulated by this result, NiO and partially graphitized carbon composite nanosheet array was synthesized in our laboratory.

In this article, NiO/C nanosheet array was successfully fabricated on Ti substrate using a two-step method. The slow release of OH^- by the hydrolysis of urea was assumed to explain the nucleation and adhesion of precursor seeds on Ti substrate. The fabrication process was simple and cheap. Furthermore, the presence of partially graphitized carbon ensured a large specific surface area and good conductivity of the final NiO/C composite. As a result, the NiO/C nanosheet array exhibited shorter response time, lower detection limit and higher sensitivity towards the

* Corresponding author. Fax: +86 027 67861185.
E-mail addresses: lixin2010@hotmail.com (X. Li), xthuang@phy.ccnu.edu.cn (X. Huang).

0022-4596/$ - see front matter Crown Copyright © 2011 Published by Elsevier Inc. All rights reserved.
doi:10.1016/j.jssc.2011.08.008

detection of glucose compared with pure NiO nanosheet. With good analytical performance, simple preparation and low cost, this NiO/C composite is promising for nonenzymatic glucose sensing.

2. Experimental

2.1. Reagents

All chemicals, including nickel acetate, urea, glucose, and sodium hydroxide (NaOH), were obtained from Sinopharm Chemical Reagent Company and used as received without further purification. All aqueous solutions were prepared in distilled water. The titanium foil was 99% pure.

2.2. Apparatus

Products were characterized by scanning electron microscopy (SEM; JSM-6700 F, 5.0 kV), powder X-ray diffraction (XRD; Bruker D-8 Avance, Cu $K\alpha$ radiation, 1.5418 Å), Raman spectroscopy (Confocal Raman Microspectroscopy, RM-1000, 514.5 nm), transmission electron microscopy (TEM; JEM-2010FEF, 200 kV), and Nitrogen adsorption–desorption measurements (Micromeritics Tristar 3000 analyzer).

All electrochemical experiments including electrochemical impedance spectroscopy (EIS) were carried out using a CHI 660C Electrochemical Work Station (CH Instrument Company of Shanghai, China). A conventional three-electrode system was adopted with NiO/C nanosheet array modified Ti foil as the working electrode, Pt wire as counter electrode, and saturated calomel electrode (SCE) as the reference electrode. All potential values were referred to the SCE.

2.3. Fabrication of NiO/C or pure NiO nanosheet array on Ti foil

NiO/C nanosheet array was prepared on Ti substrate by first dissolving nickel acetate, urea and glucose in 60 ml distilled water to achieve 0.05, 0.25 and 0.01 M, respectively. Ti foils were placed vertically in the solution. The mixing solution was transferred into a 100 ml Teflon-lined stainless steel autoclave and kept at 120 °C for 10 h. The substrate was then washed, dried at 60 °C and further annealed in N_2 gas at 500 °C for 2 h. A uniform NiO/C nanosheet array film was then formed on Ti foil. Carbon in the NiO/C composite was incorporated by the hydrothermal reaction of glucose in the first mixing solution. The glucose used here could be replaced by sucrose or cellulose.

To understand the role of carbon in final composite, pure NiO nanosheet array was prepared on Ti substrate for contrast. NiO nanosheet array was prepared by first dissolving nickel acetate and urea in 60 ml distilled water to achieve 0.05 and 0.25 M, respectively. Ti foils were placed in the solution as substrate. The solution was kept at 120 °C for 10 h. Then Ti foils were washed, dried at 60 °C and further annealed in N_2 gas at 500 °C for 2 h. Pure NiO nanosheet array film was then uniformly formed on Ti foil.

2.4. Electrochemical experiments

The electrochemical behavior of the prepared electrode was investigated by cyclic voltammetry (CV). NiO/C nanosheet array modified Ti foil (NiO/C–Ti) and pure NiO nanosheet array modified Ti foil (NiO–Ti) were evaluated as the working electrode. Amperometric curves were recorded after adding the glucose solution to the electrolyte.

3. Results and discussion

3.1. Preparation and morphology of NiO/C nanosheet array grown directly on Ti substrate

NiO/C nanosheet array film was fabricated on Ti substrate in two steps, as shown in Fig. 1. According to recent report, the polymerization and dehydration of the hydroxyl group in glucose molecules under hydrothermal condition could result in a complicated mixture of organic compounds [22]. The organic compounds were transformed into partially graphitized carbon under anneal treatment in protective gas [23]. In the hydrothermal process, both urea and glucose played important roles. The hydrolysis of urea provided a source of anions during the formation of the precursor $Ni_2(OH)_2(CO_3)$ [24]. The polymerization and dehydration of glucose under hydrothermal treatment generated a mixture of organic compounds. The organic compounds uniformly coated on the precursor $Ni_2(OH)_2(CO_3)$. During the next anneal in N_2 gas, the precursor decomposed into NiO [25]. The organic compounds were transformed into a carbon shell coating on the NiO nanosheets. Different kinds of metal oxide and carbon composites were prepared using similar method [26–28]. The possible precipitation reactions were as follows:

$$CO(NH_2)_2 + H_2O \rightarrow NH_4^+ + OH^- + CO_3^{2-} \quad (1)$$

$$Ni^{2+} + OH^- + CO_3^{2-} \rightarrow Ni_2(OH)_2(CO_3)\downarrow \quad (2)$$

$$Ni_2(OH)_2(CO_3) \rightarrow NiO + H_2O + CO_2 \quad (3)$$

The typical morphology of the prepared NiO/C nanosheet array is illustrated in Fig. 2(A–C), as observed by SEM. The prepared NiO/C composite is uniformly distributed on Ti foil on a large-scale. The film consists of interconnected nanosheets with 90–120 nm thickness and lateral sizes of 600–900 nm. These nanosheets have rough surfaces. They are decorated with small sphere particles with a diameter of 60–90 nm.

The direct growth of NiO/C nanosheet array on Ti foil was ascribed to urea. The slow release of OH^- by the hydrolysis of urea aided in the nucleation and adhesion of precursor seeds on Ti substrate. To confirm this point, pure NiO nanosheet array was prepared without the additive of glucose in the first reaction solution.

The typical morphology of pure NiO nanosheet array is illustrated in Fig. 2(D and E). The structure is similar to that of NiO/C nanosheet array. However, the pure NiO nanosheets have smooth surfaces. No other materials, such as small sphere particles, are observed. These nanosheets are aligned vertically to the Ti foil, enabling robust mechanical adhesion and electrical contact of every nanosheet to the substrate. This result implies that glucose has no relationship with the direct growth of nanosheet array on Ti substrate.

In other two contrast experiments, urea was replaced by ammonia or sodium hydroxide. Nothing was obtained on Ti substrate, as observed from Fig. 2(F) and its inset. This result confirmed that urea played an important role in the direct growth

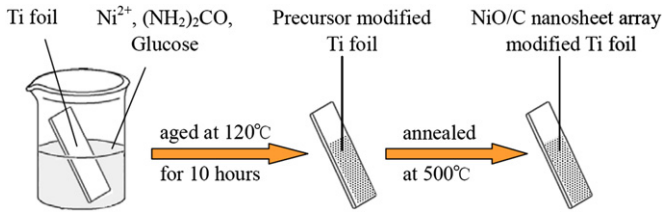

Fig. 1. Fabrication processes of the NiO/C nanosheet array film grown directly on Ti foil.

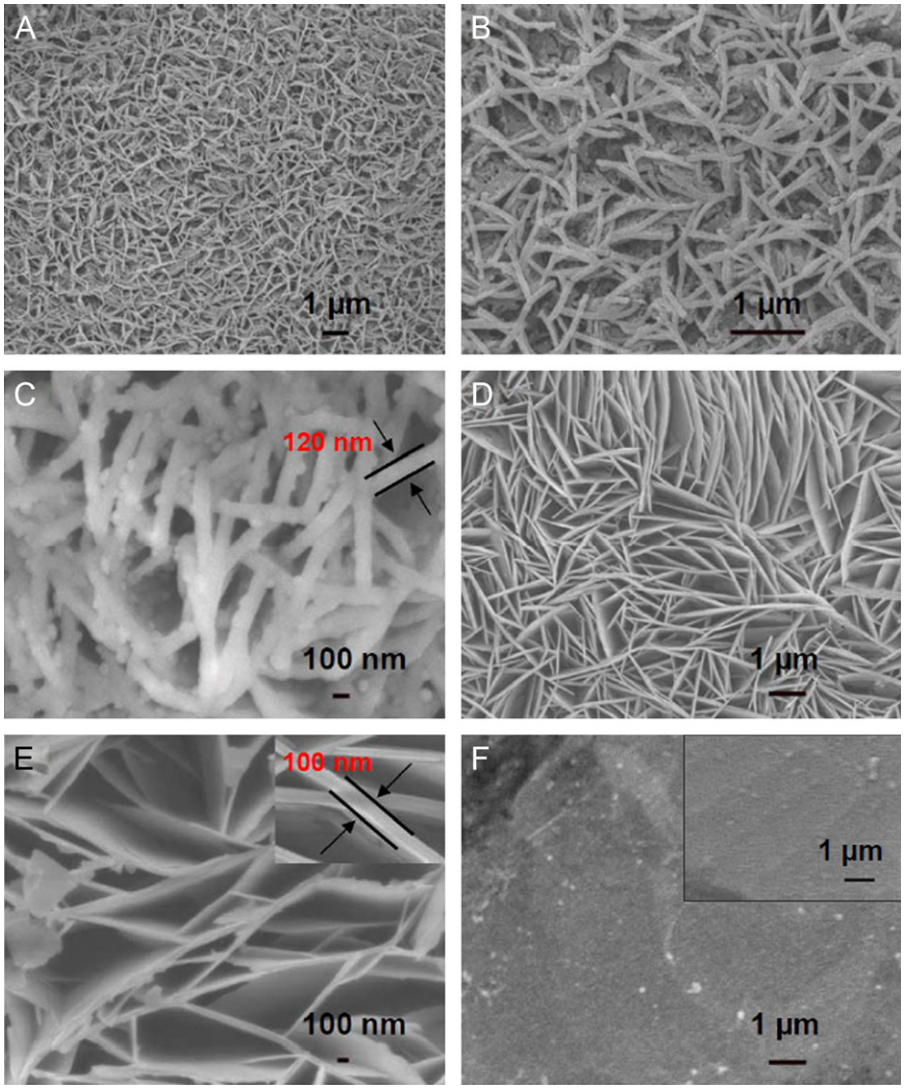

Fig. 2. (A, B and C) SEM images of NiO/C nanosheet array on Ti foil; (D and E) SEM images of pure NiO nanosheet array on Ti foil; and (F) SEM image of Ti foil after the reaction using ammonia as precipitation reagent, inset: SEM image of Ti foil after the reaction using sodium hydroxide as precipitation reagent.

of nanosheet array on Ti substrate. Using ammonia or sodium hydroxide as precipitation reagent, the OH^- was abundant in the solution. The nucleation and growth of precursor rapidly occurred in the solution. The coprecipitation reaction was so fast that it was hard for precursor seeds to adhere on Ti substrate. Using urea as precipitation reagent, the OH^- was gradually released by the hydrolysis of urea. The coprecipitation reaction was relatively mild that it was possible for precursor seeds to adhere on Ti substrate. As a result, a uniform nanosheet array film was formed on the Ti foil.

3.2. *Structure characterizations of NiO/C nanosheet array grown directly on Ti substrate*

The XRD pattern of NiO/C nanosheet array is presented in Fig. 3(A) showing characteristic diffraction peaks at 37.275° and 43.316°, which correspond to the (101) and (012) crystalline planes of NiO material, respectively (JCPDS file no. 44-1159). Other strong diffraction peaks can be assigned to the crystalline planes of Ti substrate (JCPDS file no. 01-1197).

Fig. 3(B) shows the Raman spectra with two strong peaks at 1369 (D band) and 1598 cm^{-1} (G band), which are due to the disordered defects of the carbon material and relatively high graphitization degree, respectively. This confirms the presence of partial graphitized carbon in the final composite. Unlike other complex preparation methods, carbon in the composite is incorporated through the hydrothermal reaction of glucose in the first mixing solution. This method has been proven to be simple, cheap, and effective.

The structure of NiO/C composite is further investigated by TEM. One piece of platelet examined is shown in Fig. 3(C). The nanosheet is actually composed of small NiO nanoparticles with numerous pores in the structure. As indicated by arrows in Fig. 3(D), NiO nanoparticles are homogeneously surrounded by a carbon shell. The carbon shell offers a conductive network for NiO nanoparticles that facilitates the charge transport. The inset of Fig. 3(D) shows the corresponding selected-area electron diffraction pattern of NiO in the composite.

Porous nanomaterials are more attractive in the detection of glucose. Their large specific surface area can effectively increase the adsorption of glucose. In order to investigate the porosity of NiO/C nanosheet array, nitrogen adsorption–desorption isotherm and BET analysis were performed and compared to that of the pure NiO nanosheet. As shown in Fig. 4(A), both NiO/C and pure NiO nanosheet array exhibit distinct hysteresis loop, indicating their porous structure. The N_2 uptakes of the initial part for the

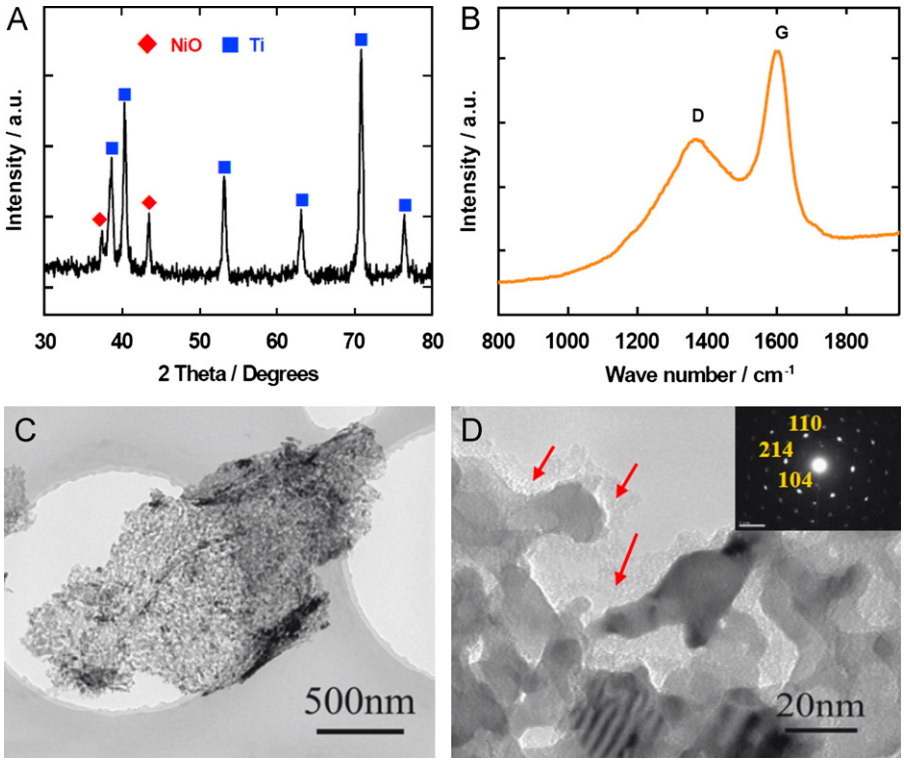

Fig. 3. (A) XRD pattern; (B) Raman spectra; (C and D) TEM images of NiO/C nanosheet, inset: selected-area electron diffraction pattern of the NiO/C composite.

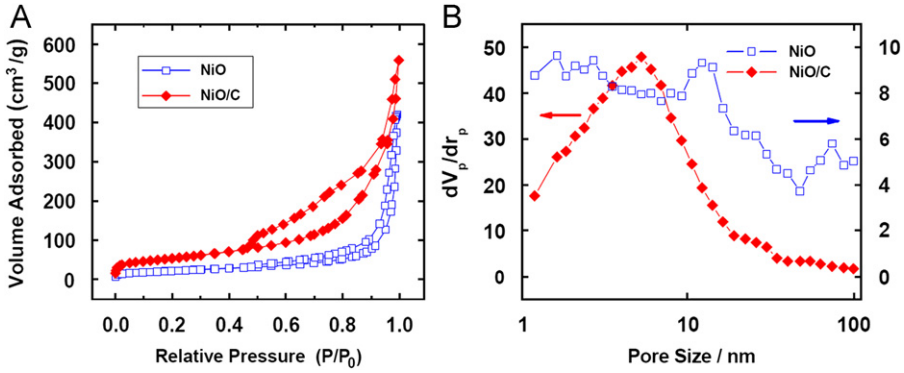

Fig. 4. (A) Nitrogen adsorption–desorption isotherm and (B) pore-size distribution of pure NiO and NiO/C nanosheet.

two isotherms are very low, indicating the micro-pores may be ignored in the two samples. The isotherm of NiO nanosheet belongs to a mixed type in the IUPAC classification [29]. The part of isotherm at high relative pressure $P/P_0 > 0.8$ corresponds to type II, typical of non-porous or macro-porous materials. A hysteresis loop can be seen in the range $P/P_0 > 0.6$, associated with capillary condensation in meso-pores, which is characteristic of type IV isotherms. The isotherm of NiO/C composite nanosheet also belongs to a mixed type of II and IV with a hysteresis loop of type H3. The hysteresis loop is bigger than that of NiO nanosheet, indicating the higher meso-porosity of NiO/C composite nanosheet sample.

Fig. 4(B) gives the plot of the pore size distribution of NiO/C and pure NiO nanosheet array. Both of them contain small micro-pores (<2 nm), meso-pores (from 2 to 50 nm) and macro-pores (>50 nm). The average pore diameter of NiO/C nanosheet is 15.8 nm, smaller than that of pure NiO nanosheet (29.7 nm). The calculated BET surface areas of NiO and NiO/C nanosheet are 79.6 and 194 m^2/g while their pore volumes are 0.59 and 0.76 cm^3/g, respectively. The presence of carbon obviously increases the specific surface area of NiO/C composite. This improvement is valuable for the enhancement of sensitivity towards the detection of glucose.

3.3. Amperometric determination of glucose at NiO–Ti and NiO/C–Ti electrode

Fig. 5(A) shows the CV curves of the prepared NiO–Ti and NiO/C–Ti electrode in 0.1 M NaOH solution at scan rate of 0.10 V/s. Both of them exhibited a pair of redox peaks. The redox peak potentials at 0.41 V and 0.31 V were assigned to the Ni^{2+}/Ni^{3+} redox couple formation in the alkaline medium [30].

The EIS results presented in Fig. 5(B) show that the electron transfer resistance at the NiO/C–Ti electrode is about 134 Ω (the diameter of semicircle), much smaller than that of the NiO–Ti electrode (~332 Ω), indicating its improved conductivity. The conductivity of the NiO/C composite is obviously improved due to the incorporation of carbon.

Fig. 6(A and B) give the detection limit and response time of NiO–Ti and NiO/C–Ti electrode under desired potential of 0.41 V.

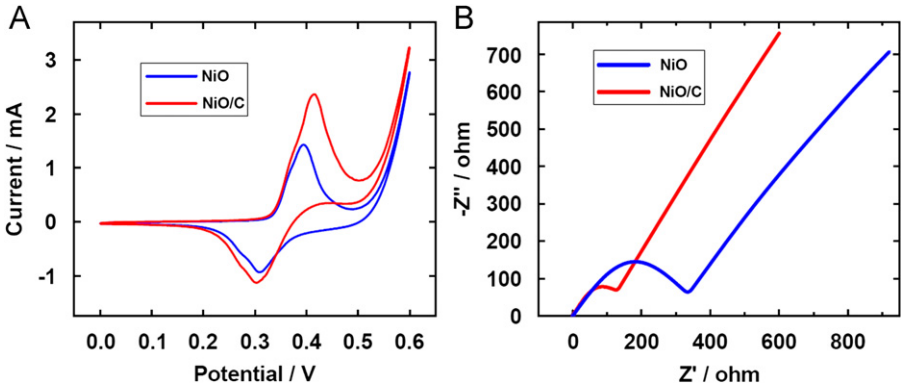

Fig. 5. (A) CV curves of NiO–Ti (lower curve) and NiO/C–Ti (upper curve) electrode recorded 0.1 M NaOH solution at a scan rate of 0.10 V/s; (B) EIS measurements of 5 mM $[Fe(CN)_6]^{3-/4-}$ in 0.1 M KCl using NiO–Ti and NiO/C–Ti electrodes.

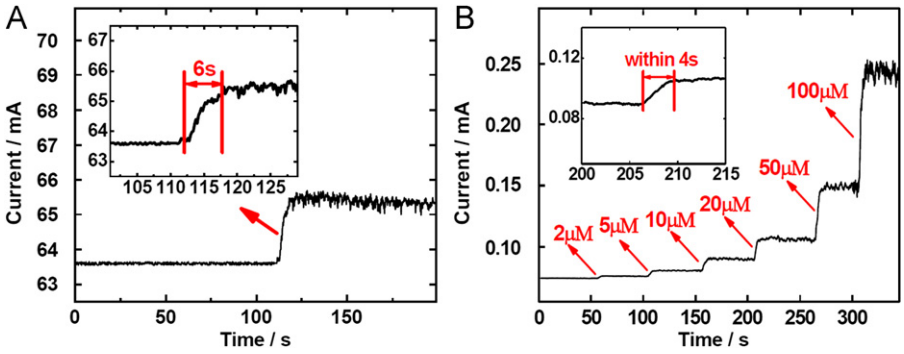

Fig. 6. (A) Detection limit of NiO–Ti electrode, inset: response time at 6 s; and (B) current–time response of NiO/C–Ti electrode with an addition of low concentration glucose solution, inset: response time within 4 s.

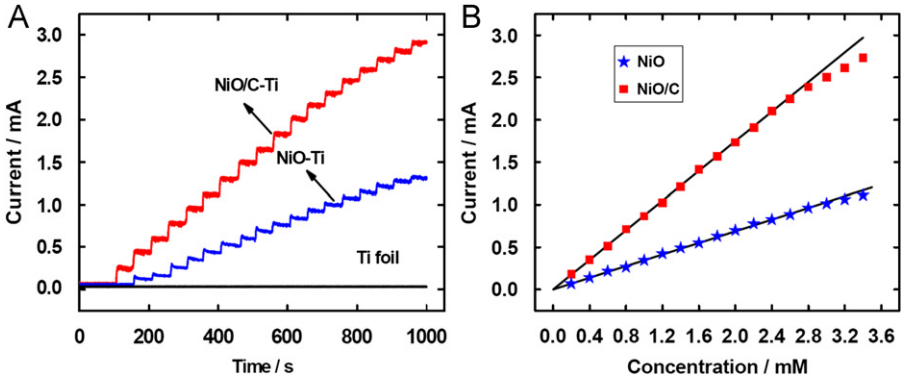

Fig. 7. (A) Current–time curves of Ti foil, NiO–Ti and NiO/C–Ti electrodes obtained at 0.41 V with the successive addition of same concentration glucose solution; and (B) corresponding calibration curves of glucose concentration on NiO–Ti and NiO/C–Ti electrodes.

The detection limit of the NiO–Ti electrode is at 5 μM and the response time is 6 s. The NiO/C–Ti electrode exhibits better performance. Fast response time within 4 s is observed and the detection limit is at 2 μM at a signal-to-noise ratio of 3. In addition, the NiO/C–Ti electrode exhibits a linear response with the addition of low concentration glucose solution.

Fig. 7(A) presents the current–time curves of NiO–Ti electrode and NiO/C–Ti electrode with successive additions of glucose. Each injection increased the glucose concentration at a 0.2 mM step. The glucose molecule contained aldehyde group (–CHO). The aldehyde group could be generally oxidized to a carboxyl group (–COOH). The oxidation mechanism of glucose by Ni-based materials could be represented by the following reactions:

$$Ni^{2+} + OH^- \rightarrow Ni^{3+} + e^- \quad (4)$$

$$Ni^{3+} + Glucose \rightarrow Ni^{2+} + Gluconic\ acid \quad (5)$$

First, Ni^{2+} could be electro-oxidized to Ni^{3+} in alkaline solution. In this process, the release of electron resulted in the formation of oxidation peak current. Second, glucose ($C_6H_{12}O_6$) could be oxidized to gluconic acid ($C_6H_{12}O_7$) by Ni^{3+}. In this process, Ni^{3+} was deoxidized to Ni^{2+}. Therefore, the presence of glucose could lead to an increase in current.

Pure Ti foil exhibited no amperometric response with the addition of glucose. It was stable enough to be used as a novel substrate in electrochemistry. NiO/C–Ti electrode exhibited higher response currents than NiO–Ti electrode, indicating its better electrocatalytic oxidation activity of glucose. The corresponding calibration curves of glucose concentration are shown in Fig. 7(B). The NiO–Ti electrode exhibited a linear range up to

3.0 mM with a sensitivity of 229.3 μAm M^{-1} cm^{-2} (R^2=0.99906). The NiO/C–Ti electrode exhibited a higher sensitivity at 582.6 μ Am M^{-1} cm^{-2} (R^2=0.99961). Its linear range was estimated as 2.6 mM.

NiO/C nanosheet array exhibited shorter response time, lower detection limit and higher sensitivity towards the detection of glucose. The presence of carbon ensured a large specific surface area and good conductivity of the final composite. The large specific surface area increased the adsorption of glucose. The good conductivity facilitated the electron transfer. The fast electron transfer was helpful in shortening the response time and enhancing the sensitivity. Therefore, the NiO/C nanosheet array exhibited better catalytic oxidation activity of glucose over the pure NiO nanosheet. Compared to other nonenzymatic glucose sensors, the proposed NiO–Ti electrode showed good performance in terms of sensitivity and stability. For example, it exhibited higher sensitivity than sensors based on carbon materials [31–33], nanoscale $Ni(OH)_2$ [34] and NiO/MCNTs composite [35]. The electrode maintained at least 93.6% of the initial sensitivity even after 60 days. The electrode exhibited long-term stability in the duplicative determination of glucose. This result indicated that an effective glucose sensor based on NiO/C nanocomposite can be easily prepared using our method.

4. Conclusion

NiO/C nanosheet array was fabricated on Ti foil for the first time. The direct growth of nanosheet array on electrode surface improved the adhesion of electrocatalyst to the substrate. No extra binder was used in the fabrication of electrode, offering advantages of simplicity and economy. Moreover, the presence of carbon ensured a large specific surface area and good conductivity of NiO/C nanocomposite. As a result, the NiO/C nanosheet array exhibited better catalytic oxidation activity of glucose over the pure NiO nanosheet array. As a glucose sensor, the proposed electrode exhibited high sensitivity, fast response, good stability, and appropriate linear range. Combined with the merits of NiO/C nanosheet array on a conductive substrate, this composite electrode is promising for nonenzymatic glucose sensing.

Acknowledgment

This work was financially supported by the National Natural Science Foundation of PR China (No. 50872039).

References

[1] J. Wang, Chem. Rev. 108 (2008) 814–825.
[2] J. Shah, E. Wilkins, Electroanalysis 15 (2003) 157–167.
[3] J.M. Zen, C.W. Lo, Anal. Chem. 68 (1996) 2635–2640.
[4] X. Han, Y. Zhu, X.L. Yang, C.Z. Li, J. Alloys Compd. 500 (2010) 247–251.
[5] R. Wilson, A.P.F. Turner, Biosens. Bioelectron. 7 (1992) 165–185.
[6] S. Park, H. Boo, T.D. Chung, Anal. Chim. Acta 556 (2006) 46–57.
[7] Y. Li, Y.Y. Song, C. Yang, X.H. Xia, Electrochem. Commun. 9 (2007) 981–988.
[8] X.H. Kang, Z.B. Mai, X.Y. Zou, P.X. Cai, J.Y. Mo, Anal. Biochem. 363 (2007) 143–150.
[9] F.J. Miao, B. Tao, L. Sun, T. Liu, J.C. You, L.W. Wang, P.K. Chu, Sens. Actuators B 141 (2009) 338–342.
[10] L.R. Kong, X.F. Lu, X.J. Bian, W.J. Zhang, C. Wang, J. Solid State Chem. 183 (2010) 2421–2425.
[11] M. Fleischmann, K. Korinek, D. Pletcher, J. Chem. Soc., Perkin Trans. 2 (1972) 1396–1403.
[12] A. Salimi, M. Roushani, Electrochem. Commun. 7 (2005) 879–887.
[13] Q.F. Yi, W. Huang, W.Q. Yu, L. Li, X.P. Liu, Electroanalysis 20 (2008) 2016–2022.
[14] L.M. Lu, L. Zhang, F.L. Qu, H.X. Lu, X.B. Zhang, Z.S. Wu, S.Y. Huan, Q.A. Wang, G.L. Shen, R.Q. Yu, Biosens. Bioelectron. 25 (2009) 218–223.
[15] X. Cheng, S. Zhang, H.Y. Zhang, Q.J. Wang, P.G. He, Y.Z. Fang, Food Chem. 106 (2008) 830–835.
[16] Y. Liu, H. Teng, H.Q. Hou, T.Y. You, Biosens. Bioelectron. 24 (2009) 3329–3334.
[17] A. Vinu, P. Srinivasu, M. Takahashi, T. Mori, V.V. Balasubramanian, K. Ariga, Microporous Mesoporous Mater. 100 (2007) 20–26.
[18] W.D. Zhang, J. Chen, L.C. Jiang, Y.X. Yu, J.Q. Zhang, Microchim. Acta 168 (2010) 259–265.
[19] G.C. Yang, E.J. Liu, N.W. Khun, S.P. Jiang, J. Electroanal. Chem. 627 (2009) 51–57.
[20] H.S. Yin, Y.L. Zhou, Q. Ma, S.Y. Ai, Q.P. Chen, L.S. Zhu, Talanta 82 (2010) 1193–1199.
[21] X.H. Huang, J.P. Tu, C.Q. Zhang, J.Y. Xiang, Electrochem. Commun. 9 (2007) 1180–1184.
[22] M. Sevilla, A.B. Fuertes, Carbon 47 (2009) 2281–2289.
[23] X.M. Sun, Y.D. Li, Angew. Chem. Int. Ed. 43 (2004) 597–601.
[24] L.L. Wu, Y.S. Wu, H.Y. Wei, Y.C. Shi, C.X. Hu, Mater. Lett. 58 (2004) 2700–2703.
[25] P. Justin, S.K. Meher, G.R. Rao, J. Phys. Chem. C. 114 (2010) 5203–5210.
[26] H. Qiao, L.F. Xiao, Z. Zheng, H.W. Liu, F.L. Jia, L.Z. Zhang, J. Power Sources 185 (2008) 486–491.
[27] L. Zhang, W.Z. Wang, M. Shang, S.M. Sun, J.H. Xu, J. Hazard. Mater. 172 (2009) 1193–1197.
[28] J. Read, D. Foster, J. Wolfenstine, W. Behl, J. Power Sources 96 (2001) 277–281.
[29] International Union of Pure and Applied Chemistry (IUPAC), Pure Appl. Chem. 57 (1985) 603–619.
[30] E. Scavetta, M. Berrettoni, R. Seeber, D. Tonelli, Electrochim. Acta 46 (2001) 2681–2692.
[31] J.X. Wang, X.W. Sun, X.P. Cai, Y. Lei, L. Song, S.S. Xie, Electrochem. Solid-State Lett. 10 (2007) 58–60.
[32] J.S. Ye, Y. Wen, W.D. Zhang, L.M. Gan, G.Q. Xu, F.S. Sheu, Electrochem. Commun. 6 (2004) 66–70.
[33] J.C. Ndamanisha, L.P. Guo, Bioelectrochemistry 77 (2009) 60–63.
[34] A. Safavi, N. Maleki, E. Farjami, Biosens. Bioelectron. 24 (2009) 1655–1660.
[35] M. Shamsipur, M. Najafi, M.M. Hosseini, Bioelectrochemistry 77 (2010) 120–124.